JPE 17-4-26

https://doi.org/10.6113/JPE.2017.17.4.1117
ISSN(Print): 1598-2092 / ISSN(Online): 2093-4718

Utilization of Active Diodes in Self-powered Sensorless Three-phase Boost-rectifiers for Energy Harvesting Applications

Alejandro Tapia-Hernandez[†], Mario Ponce-Silva[*], Victor Hugo Olivares-Peregrino[*], Jesus Elias Valdez-Resendiz[**], and Leobardo Hernandez-Gonzalez[***]

[†]Instrumentation and Driver HMI, Continental Automotive, Guadalajara, Mexico
[*]Centro Nacional de Investigacion y Desarrollo Tecnologico, Cuernavaca, Mexico
[**]Tecnologico de Monterrey, Monterrey, Mexico
[***]Instituto Politecnico Nacional ESIME Culhuacan, Av. IPN, S/N, Mexico

Abstract

The main contribution of this paper is the use of sensorless active diodes to generate the gate signals for a three-phase boost-rectifier with a self-powered control scheme. The sensorless operation is achieved making use of the gate control signals generated by the active diode schemes on each of the switching devices using a pulse width half-controlled boost rectifier modulation technique (PWM-HCBR). The proposed scheme synchronizes the gate control signals with a three phase voltage supply. Autonomous operation is obtained making use of the output DC bus to feed the control circuitry, the active diodes and the driver circuitry. The three-phase boost-rectifier is supplied by a three-phase permanent magnet electric generator powered by a solar concentrator dish with variable voltage and variable frequency conditions. Experimental results report an efficiency of up to 94.6% for 25 W and an input of 3.6 V peak per phase with 450.

Key words: Active diodes, Boost-rectifier, Energy harvesting

I. INTRODUCTION

The use of sensorless schemes in energy harvesting applications to drive and control AC-DC single-phase and three-phase converters has been reported in several papers [1]-[6]. In AC-DC energy-harvesting applications, like solar concentrator dishes, the use of a sensorless self-powered scheme is desirable to improve the power density and efficiency of the system. However, the use of an external supply for the control circuitry can not always be avoided. For example, [7] presents a voltage doubling converter with comparators on the control circuitry. It is fed by the output voltage when it reaches the minimum required output voltage level. If this voltage is not reached, the comparators are fed with external power sources.

One of the problems with these schemes is obtaining a high efficiency with a low number of components and a reduced space. This issue is worst when the main voltage supply presents low and variable input voltage (below of 3.6 V peak) and variable input frequency conditions as is reported in [3], [8]-[15]. One example of this type of application is in solar concentrator dishes, where an electric generator is mechanicaly fed by an external combustion engine (Stirling engine) heated by the sun concentrated in the focus of a parabolic dish. Due to the movement of the sun, the system presents heat variations which result in variations of the amplitude and frequency of the output voltage waveform in the electric generator.

The three-phase boost-rectifier (TPBR) is one of the most widely used topologies employed in these applications. It employs three MOSFETs and three diodes to rectify and regulate in the same stage as the output voltage making use of different pulse width modulation techniques (PWM). The authors of [3] reported a high efficiency (93%) three-phase

Manuscript received Oct. 24, 2016; accepted May 2, 2017
Recommended for publication by Associate Editor Chun-An Cheng.
[†]Corresponding Author: alejandro.tapia.hernandez@gmail.com
Tel: +52(33)3050-1100, Ext. 8473, Continental Automotive Guadalajara
[*]CENIDET, Mexico
[**]Tecnologico de Monterrey, Mexico
[***]Instituto Politecnico Nacional ESIME Culhuacan, Mexico

© 2017 KIPE

boost rectifier with a 10 V peak input per phase by implementing a PWM technique on a Digital Signal Processor (DSP) for a 60 W application. However, when the input voltage is less than 10 V peak, the losses in the diodes are increased due to the diode voltage drop (0.7 V). As a result, the overall efficiency decreases. In [9] the diodes are changed by MOSFETs in order to improve them. This change implies the use of additional control circuitry and an external voltage supply. These additional components are necessary to drive and guarantee the synchrony between the converter and the voltage supply. For example, in [3] and [4] the source of the voltage supply is not specified for the additional control circuitry. In order to simplify the drive and control circuitry to use MOSFETS instead of diodes in the three phase boost rectifier, a self-powered (autonomous) scheme is desired in order to reduce the components and space while maintaining a high efficiency. To maintain autonomous operation, recent studies have used the output voltage of converters to self-powered the electronic circuitry (control IC and driver) [16]-[18] by making use of auxiliary low-power DC-DC converters to provide the required voltage for the control IC.

On the other hand, related to the PWM technique of the TPBR, studies have reported techniques such as PWM [9], [19] and space vector pulse width modulation (SVPWM) [3], [12]. The selection of a modulation technique impacts the number of components. For example, the use of SVPWM increases the hardware requirements with respect to the classical PWM techniques. SVPWM can increase the energy consumption depending on the integrated circuit (IC) employed. These ICs can include microcontrollers (MCU), field programmable gate arrays (FPGA), digital signal processors (DSP) and digital signal controllers (dsPIC).

The main contribution of this paper is the proposal of an autonomous sensorless scheme to generate the gate signals of a three-phase boost-rectifier to synchronize it with a three-phase permanent magnet electric generator for energy-harvesting applications making use of a modified active diodes scheme to avoid the use of additional sensors allowing for a high efficiency due to the employed modulation technique. Fig. 1(a) shows the proposed scheme with a self-powered configuration for the control stage and drivers with sensorless operation. This can then be compared with a traditional three-phase scheme which make use of different sensors in order to guarantee synchrony with the voltage supply (Fig. 1b). Making use of the proposed sensorless scheme, it is possible to simplify the control and driver of the three-phase boost rectifier reducing the number of components and obtaining a high efficiency of almost 95% due to the employed modulation technique.

The structure of this paper is as follows. In section II, an analysis of the topology with the autonomous sensorless scheme is presented. In section III, the design methodology is described. Section IV shows experimental results obtained with the design, and section V has a discussion of the experimental results from section IV.

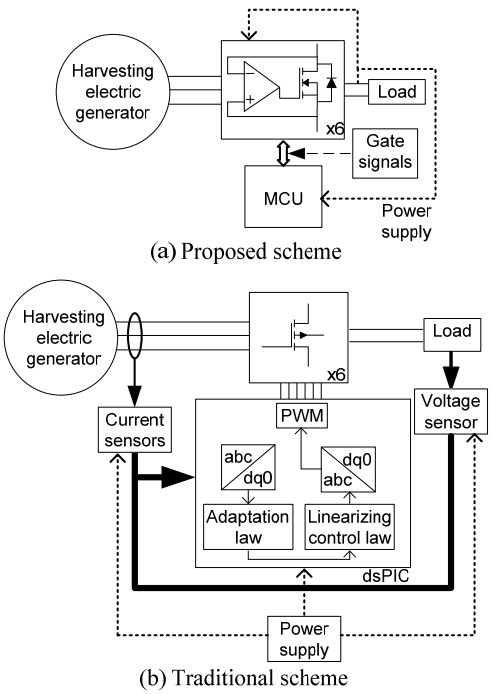

Fig. 1. Comparative between: (a) the proposed and (b) the traditional self-powered sensorless schemes.

II. ANALYSIS OF THE TOPOLOGY

In AC-DC energy harvesting applications, the main challenge is to a get high efficiency power conversion with output voltage regulation along with even variable frequency and input voltage conditions. The TPBR consists of the integration of a single-stage of a three-phase rectifier in series with a boost converter as shown in Fig. 2(a). First this topology rectifies the AC input voltage and then the boost converter regulates the output voltage. The main problem of the topology shown in Fig. 2(a), when it is used in energy harvesting applications, is its low efficiency due to the diode voltage drop (0.7 V) of the three-phase rectifier [4]. Recent studies have reported bridgeless topologies to rectify and regulate the output voltage at the same time, such as those shown in Fig. 2(b) and 2c [3]. Fig. 2(b) shows a TPBR which makes use of diodes and MOSFETs to rectify and regulate the output voltage. It only implements PWM for the MOSFETs in order to simplify the control circuitry to improve the efficiency. In Fig. 2(c), an active three-phase PWM rectifier is shown. It employs six MOSFETs with PWM increasing the efficiency. However, the control circuitry is more complex. In order to maintain a high efficiency with control simplicity, the proposed scheme makes use of active diodes and MOSFETs as is shown in Fig. 2(d).

The TPBR employed in Fig. 2(d) works with 3 boost converters with six operating modes. The upper MOSFETs

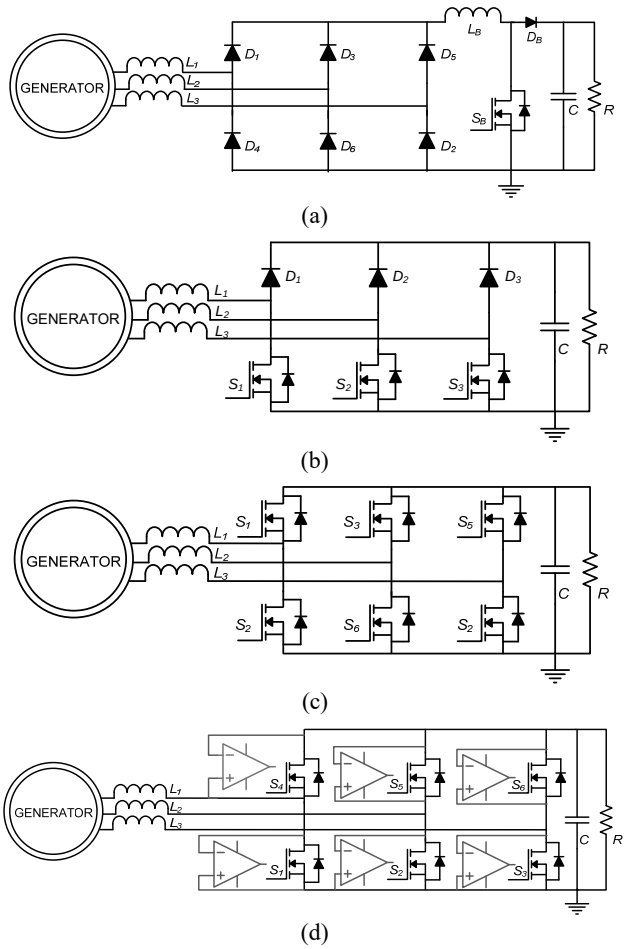

Fig. 2. (a) Three-phase rectifier in series with a boost converter; (b) three-phase boost-rectifier with the HCBR; (c) three-phase active rectifier and; (d) three-phase boost-rectifier with the active diodes scheme.

work like the freewheeling diodes of typical boost converters and the lower MOSFETs work with PWM modulation to step-up the output voltage. The operating sequence of the devices is a function of the input line voltage from the electric generator. In the next section, the operating modes of the TPBR are described.

A. Operating Modes with the PWM HCBR Modulation Technique in the steady-state operation of a TPBR

The employed TPBR (Fig. 2(d)) works with the pulse width half controlled boost rectifier modulation technique (PWM HCBR), which offers a simple drive and generation of the control signals of the switches for keeping a high efficiency [3]. The PWM HCBR modulation technique consider that only the low-side devices of the three-phase boost-rectifier converter work with PWM, while the upper-side devices are only considered as diodes with low losses. The bottom devices work in three different modes (on-mode, off-mode and PWM mode) depending of the phase voltage sequences, as is indicated in Fig. 3. Each mode works during 120° of each of the supply phase voltage waveforms.

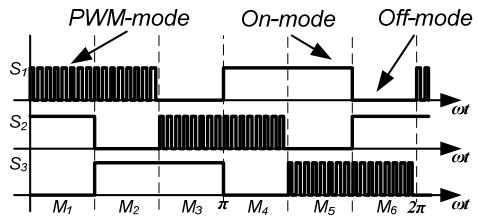

Fig. 3. Half-controlled boost-rectifier modulation waveforms and operating modes.

This modulation has been thoroughly described in [3] and it uses space vector analysis to generate the control signals.

Fig. 3 shows control signals for the low-side devices of a three-phase boost-rectifier operating with PWM HCBR modulation. From Fig. 3, six operating modes (M_1-M_6) are used to describe the operation of the converter. The equivalent circuits for the six operating modes of the three-phase boost-rectifier are shown in Fig. 4, and are described as follows:

Mode 1: during this operating mode S_1 is PWM modulated similar to the boost converter, the output voltage is regulated by the duty cycle. When S_1 is on (t_{on}=DT_S), S_4 turns off (t_{on}=$(1-D)T_S$); and when S_1 is off, S_4 turns on. This is similar to a boost converter. S_4 works in the free-wheeling mode due to the PWM operation of S_1. During this mode, S_2 remains on (t_{on}=T_S) to achieve an efficient current conduction path for the line voltage v_{in}=v_{AB} instead of the parasitic diode of S_2.

Mode 2: S_1 and S_4 hold their operation, and only S_2 and S_3 change their operating conditions. S_2 remains off (t_{on}=0) and S3 remains on (t_{on}=T_S) to achieve the line voltage v_{in}=v_{AC} that supplies the boost-rectifier instead the parasitic diode of S_3. This means that phase C provides energy to the load while phase B does not.

Mode 3: in this mode S_1 turns off and S_2 starts working with PWM modulation. S_3 is still on (t_{on}=T_S) to achieve an efficient conduction path to the line voltage v_{in}=v_{BC} instead of the parasitic diode of S_3. Phase B stops supplying energy and phase A starts supplying energy to the load. S_5 starts working in the free-wheeling mode due to the PWM operation of S_2. When S_2 is on (t_{on}=DT_S), S_5 turns off (t_{on}=$(1-D)T_S$); and when S_2 is off, S_5 turns on. This is similar to a boost converter.

Mode 4: S_2 and S_5 hold their operation, S_3 turns off (t_{on}=0) and S_1 turns on (t_{on}=T_S) to supply energy to the line voltage v_{in}=v_{BA} instead the parasitic diode of S_1. The energy path is opposite that of mode 1.

Mode 5: S_3 starts working with the PWM modulation. S_1 (t_{on}=T_S) continues supplying the line voltage v_{in}=v_{CA} instead the parasitic diode of S_1, and S_2 turns off. The energy flux is opposite that of mode 2. S_6 starts working in the free-wheeling mode due to the PWM operation of S_3. When S_3 is on (t_{on}=DT_S), S_6 turns off (t_{on}=$(1-D)T_S$); and when S_3 is off, S_6 turns on. This is similar to a boost converter.

Mode 6: S_3 and S_6 hold their operation. S1 turns off (ton=0) and S_2 turns on (t_{on}=T) supplying the line voltage v_{in}=v_{CB}

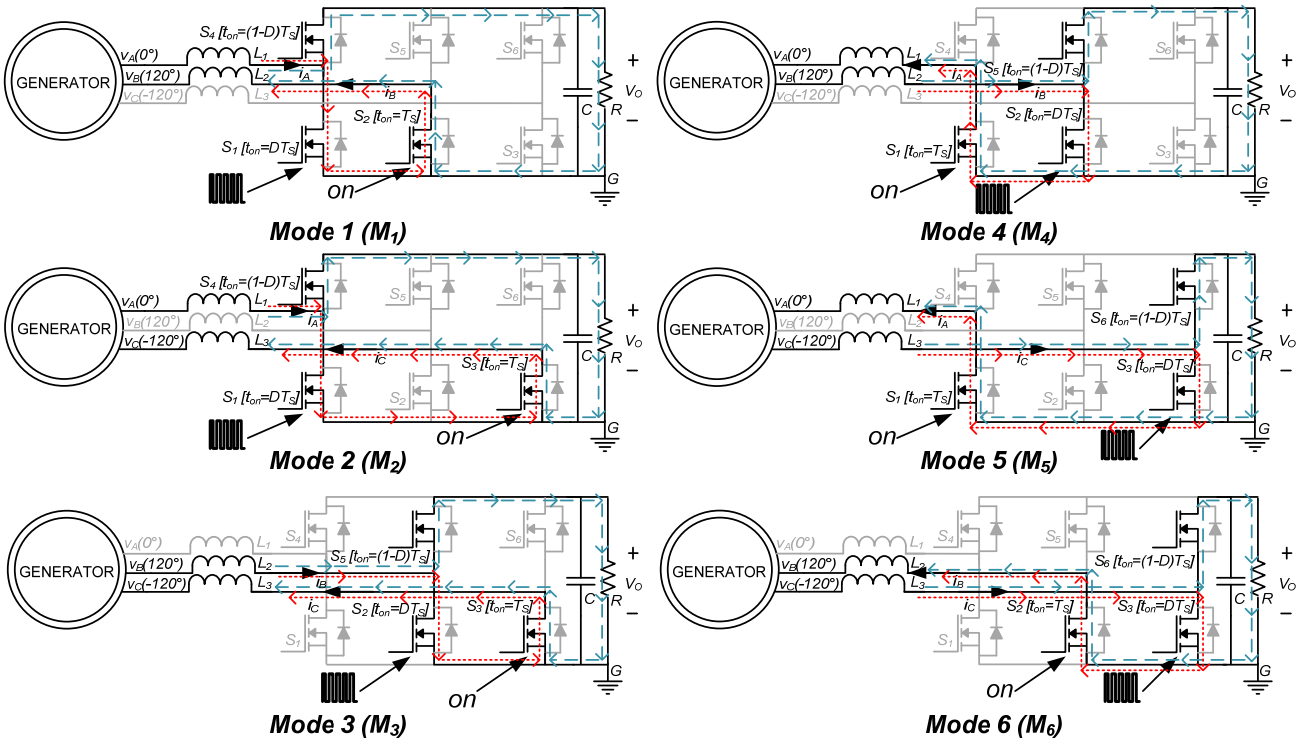

Fig. 4. Operating modes of a three-phase boost-rectifier with the PWM HCBR modulation.

instead the parasitic diode of S_2. The operation is opposite to that of mode 3.

As can be noted in Fig. 3 and Fig. 4, the analysis of the three-phase boost-rectifier can be simplified to a single boost converter analysis since it emulates six different single boost converters with six different line voltages from the three-phase electric generator (v_{AB}, v_{AC}, v_{BC}, v_{BA}, v_{CA}, v_{CB}). In the same way, the operating devices are a function of the supply line voltage of the three-phase electric generator and the control waveform of the PWM HCBR modulation.

B. Sensorless Operation with the PWM HCBR Modulation

The proposed sensorless scheme is based on active diodes (a voltage comparator with a MOSFET) [20]. It works as follows. The output voltage from each voltage comparator changes to a high level when the voltage on its positive input is higher than the voltage on its negative input; and it changes to a low level when the opposite occurs.

Therefore, the MOSFET works like a diode with efficiency improvement. The advantage of the proposed sensorless scheme is to simplify the analysis and implementation of the PWM HCBR modulation for a three-phase boost-rectifier. The proposal uses gate signals from the MOSFETs (the output voltage from voltage comparators) to synchronize the three-phase boost-rectifier with an electric generator following the trigger conditions shown in Table I and Fig. 5. Using these trigger conditions, it is possible to implement a synchronized PWM HCBR modulation without additional voltage or current sensors like those used in other works.

TABLE I
TRIGGER CONDITIONS FOR THE WORKING MODES OF MOSFETS

Device	Trigger condition
S_1	PWM mode: S_4 High level mode: S_1 Low level mode: $S_3S_5 \| \| S_2S_6$
S_2	PWM mode: S_5 High level mode: S_2 Low level mode: $S_3S_4 \| \| S_1S_6$
S_3	PWM mode: S_6 High level mode: S_3 Low level mode: $S_2S_4 \| \| S_1S_5$

Fig. 6 shows steady-state waveforms for a three-phase boost-rectifier working with the PWM HCBR modulation. Because of the behavior of the employed active diodes and the PWM mode on the low-side devices, there is an initial trigger on the output voltage of the upper voltage comparators due to the parasitic diode on the MOSFET. This causes S_4, S_5 and S_6 to turn on for a short period of time, T_1.

For example, S_6 turns on due to the higher voltage on the positive input of its voltage comparator with respect to the rectified voltage on the negative input. This transition is used as a trigger condition to activate the PWM mode on S_3. After this short period of time (T_1), the voltage waveform on the superior diodes is the complemented PWM waveform on S_3 along T_2 like the free-wheeling diode behavior of boost converters. This behavior is similar for S_1-S_6. The v_0 waveform shown in Fig. 6 has two frequency ripples. The low frequency ripple is due to the input voltage frequency, and the high frequency ripple due to the switching frequency of the

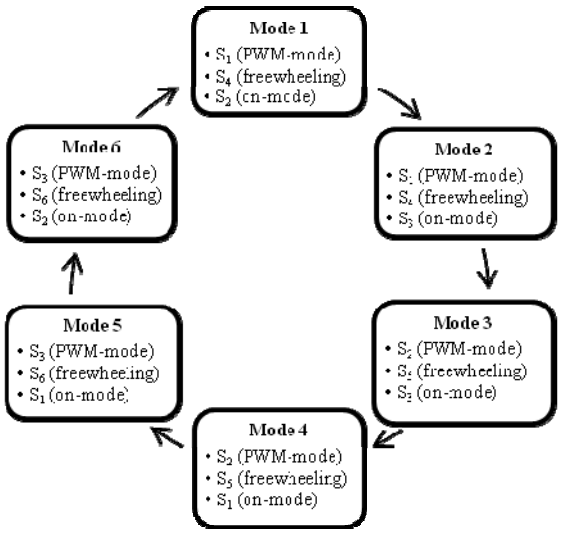

Fig. 5. Flow chart of the trigger condition changes between the operating modes (M_1 to M_6) of a three-phase boost-rectifier with the PWM HCBR modulation.

converter. v_{AN}, v_{BN} and v_{CN} are the AC input voltages per phase referred to the neutral; and v_{AG}, v_{BG} and v_{CG} are the AC input voltages per phase referred to the ground. Due to this, the negative part of the waveform is neglected and the switching frequency is visible.

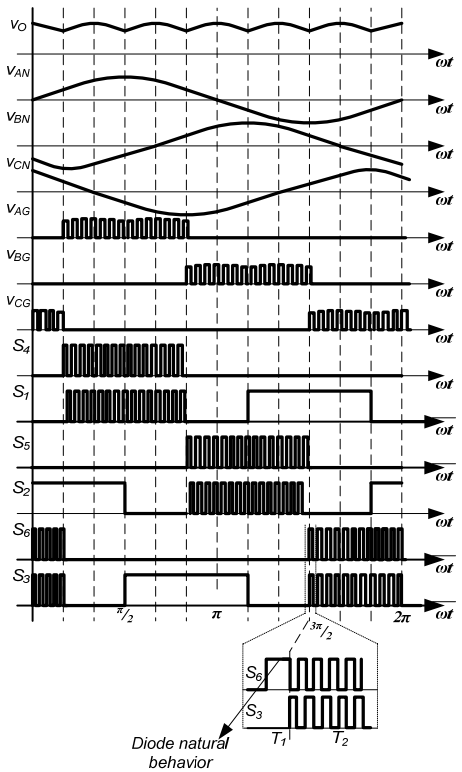

Fig. 6. Steady-state waveforms for a three-phase boost-rectifier with the PWM HCBR modulation.

III. Design Procedure

The design procedure for the PWM HCBR steady-state operation is divided into three parts: the three-phase boost-rectifier design including the voltage behavior of employed the permanent magnet electric generator, the control circuitry design with the autonomous active diodes scheme and the self-powering operating condition to start working as a TPBR.

A. Three-Phase Boost-Rectifier Design

The proposed operating conditions are for an autonomous energy harvesting application making use of a permanent magnet three-phase electric generator with a Y configuration. The Y configuration has a higher output voltage level with respect to the delta configuration. A higher voltage is desirable for energy harvesting applications due to the low induced output voltage on electric generators. A nominal supply peak voltage (V_{pk}) of 3.6 V was chosen because it is not common to use voltages higher than 10 V for harvesting applications with permanent magnet generators [21]-[24]. In the same way, the nominal frequency (f_L) employed to feed the converter was chosen as 450Hz ± 100 Hz in accordance with typical energy harvesting applications with input frequencies up to 1000 Hz [25]-[27]. Table II shows the proposed operating conditions of the three-phase boost-rectifier for autonomous operation in energy harvesting applications. To develop the design equations of a three-phase boost-rectifier with PWM HCBR modulation, six boost converters with six AC supply sources

TABLE II
Operating Conditions

Parameter	Variable	Value
Peak supply voltage per phase of the electric generator	v_{pk}	*3.6 V*
Output voltage	v_O	*12 V*
Capacitor voltage ripple	ΔV_C	*10% v_0 = 1.2 V*
Inductor current ripple	$\Delta I_{L1,L2,L3}$	*10% i_S = 200 mA*
Output power	P_0	*25 W*
Supply frequency	f_L	*1 Hz – 900 Hz*
Switching frequency of power converter	f_{sw}	*100 kHz*
Electric generator configuration	-	*Star (Y)*

are considered. In a lot of energy harvesting applications, the environmental conditions can change the steady state operation of a system. For this reason, the power converter must have the capability to work in a wide range of supply voltages and frequencies. The operative duty cycle range (D) is a function of the input voltage per phase. According to [27] a maximum D of 75% is recommended, because a higher value can increase the losses on the inductor.

Boost converter equations are used considering a three-phase supply with a Y connection. The use of a Y connection on a three-phase electric generator has the advantage of producing

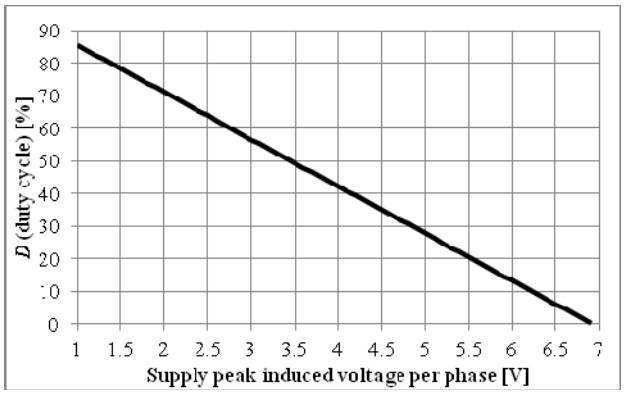

Fig. 7. Duty cycle (D) as a function of the supply peak induced voltage per phase.

an increment in the line voltage amplitude by $\sqrt{3}$ with respect to the phase voltage. Under these conditions, the output voltage level is obtained as follows:

$$v_0 = \frac{\sqrt{3}\left(v_{pk}\right)}{1-D} \tag{1}$$

Equation (2) shows the behavior of the peak induced voltage per phase as a function of the speed of the electric generator. Due to its construction, the generator has a ratio of 0.1 Hz per RPM. The permanent magnet electric generator employs three lines of magnets with different sizes. These values (r_1-r_3 and L_1-L_3) are employed to calculate the peak induced voltage per phase together with the number of turns per winding (n), the magnetic flux density (B) and the speed (rpm). The values employed for the calculation are: n=31, B=0.05307T, speed from 1 to 900 rpm, r_1=0.1069m, r_2=0.08m, r_3=0.05454m, L_1=0.054m, L_2=0.036m, and L_3=0.024m.

$$v_{pk} = \frac{3rpm(4n\pi B)}{60\sqrt{2}}\left(r_1L_1 + r_2L_2 + r_3L_3\right) \tag{2}$$

Fig. 7 shows the D necessary to keep a 12 V output voltage making use of the peak induced voltage per phase calculated in equation (2) and equation (1). As suggested in Fig. 7, the minimum input peak voltage range per phase to keep D below of 75% is 1.7 V_{pk}. This value according to equation (2) is obtained with a speed of 2500 RPM.

In the other side, a minimum D of 20% is desirable according to [27], which achieved with a 5.5 V_{pk} input at 7500 RPM. To calculate the minimum input inductance value, it is considered that during an operating mode there are two inductors present on the converter. The inductors calculation considers a maximum input current ripple ($\Delta I_{L1,L2,L3}$) of 200 mA. For this reason, the minimum inductance value is obtained as follows:

$$L_{1,2,3} \geq \frac{\sqrt{3}\left(v_{pk}\right)}{4\Delta I_L}DT_S \tag{3}$$

where T_s represents the period of f_{sw} (100 kHz). The capacitor and load resistance calculations do not change with respect to the traditional boost converter. The calculations to achieve a maximum output voltage ripple (ΔV_C) of 1.2 V and a 25 W output power are as follows:

$$C \geq \frac{P_0}{v_0\Delta v_C}DT_S \tag{4}$$

$$R = \frac{v_0^{\,2}}{P_0} \tag{5}$$

According to the operating conditions shown in Table II and making use of equations (1)-(5), the obtained values for the components are shown in Table III.

TABLE III
COMPONENT VALUES FROM THE DESIGN EQUATIONS

Component	Value
Input inductors L_1, L_2 and L_3.	*≥ 37.41 μH*
Output capacitor C	*≥ 8.33 μF*
Output Load R	*5.76 Ω*

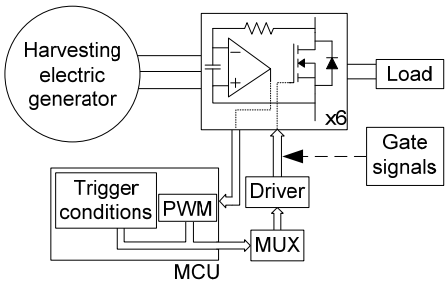

Fig. 8. Three-phase boost-rectifier using the active-diodes sensorless scheme for synchrony.

B. Active Diodes and Control Circuitry Design

The prototype implementation follows the scheme shown in Fig. 8. In order to implement the PWM HCBR modulation, the control scheme is as follows: active diodes generate gate control signals that are monitored by a MCU, the MCU implements PWM waveform and control signals to the MUX. Complete PWM HCBR modulation is obtained by making use of the signals from the MCU and MUX, and then sending them to MOSFETs trough the drivers. An advantage of the proposed autonomous synchrony scheme is its immunity to voltage unbalance on an electric generator when a closed output voltage loop is implemented. This is due to the operating scheme of the control. For each input voltage phase, the duty cycle can be corrected for an optimal output voltage regulation. The active diode topology follows a typical three-phase rectifier commutation sequence based on the device gate signals. This means that an imbalance condition on the phase voltage only modifies the PWM duty cycle for the working MOSFET but does not affect the activation sequence. Only the presence of a null phase voltage can change the operation of the proposed scheme. An input frequency (f_L) from 1 Hz to 900 Hz allows for the use of a wide range of comparators.

TABLE IV
COMPONENTS SELECTION

Component	Manufacturer part	Characteristics
MOSFETs	SiZ910 (Dual channel)	$R_{DS(on)}$ = 7.5 mΩ, 30 V 40 A
Diodes	PMEG3050EP	V_f = 314 mV
Voltage comparators	TLV3702	2.7 V - 16 V, 10 mA
MCU	Microchip PIC 16F1503	8 bits, 30 µA/MHz, 2.3 V - 5.5 V
Input inductor	WE 744 363 4700	47 µH, 8.5 A R_{ON} = 12.20 mΩ
Output capacitors	C1206C225K5RAC	2.2 µF, 50 V
DC-DC converter for control circuitry	OKI-78SR-5/1.5-W36	Fixed output 1.5 A, 5 V.

However, their supply characteristics are restrictive. To maintain autonomous three-phase boost-rectifier operation it is necessary that comparators work from 3.02 V to 12 V and preferable with a low energy consumption to improve efficiency.

MCU selection is a function of three key features: low energy consumption, low input voltage operation and the number of ports with PWM internal blocks. The selected MCU was a Microchip PIC 16F1503. It has low energy consumption with full PWM functionality. The selection of the MOSFETs is important to guarantee optimal operation with a high efficiency. The selected SiZ910 is automotive grade, which means that the package is thermally improved and the internal leakage components are reduced. In addition, its dual channel package helps to improve the power density of the converter, which reduces common ringing problems. In order to maintain the self-powering operation of the TPBR, a DC-DC converter fed by the output voltage was used to regulate the supply voltage of the control circuitry. Selected devices employed for experimental results are shown in Table IV.

C. Self-Powering Operating Condition

Due to the energy harvesting application, is common to have variable input voltage and frequency conditions. For this reason is necessary to define the boundary voltage level which determines the self-powering operation of the TPBR. At the beginning, the topology works as a three-phase rectifier, like the one developed in [28]. The output voltage (V_O) is given by equation (6) due to the Y connection.

$$v_0 = \frac{3\sqrt{3}\left(v_{pk}\right)}{\pi} \tag{6}$$

It is considered that V_O = 5 V is the minimum output voltage to guarantee the turn-on of the auxiliary DC-DC supply for the control circuitry. Then from (6) the minimum voltage peak per phase (V_{pk}) is V_{pk} =3.02 V, which represents the boundary voltage to change the power converter operation between the three-phase rectifier and the three-phase boost-rectifier. While output voltage is below V_O < 3.02V, the MOSFET parasitic diodes work like a three-phase rectifier. However, over V_O > 3.02 V, the control circuitry is turned-on and the PWM HCBR is implemented. In the next section, experimental results are shown making use of the proposed autonomous sensorless scheme with the developed prototype.

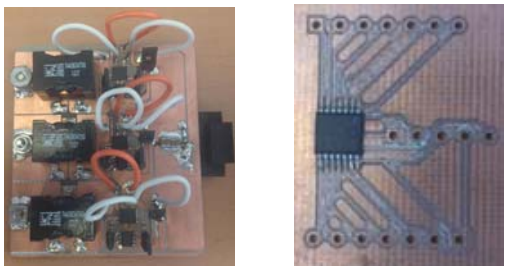

(a) (b)

Fig. 9. (a) Three-phase boost-rectifier prototype and (b) the employed PIC 16F1503.

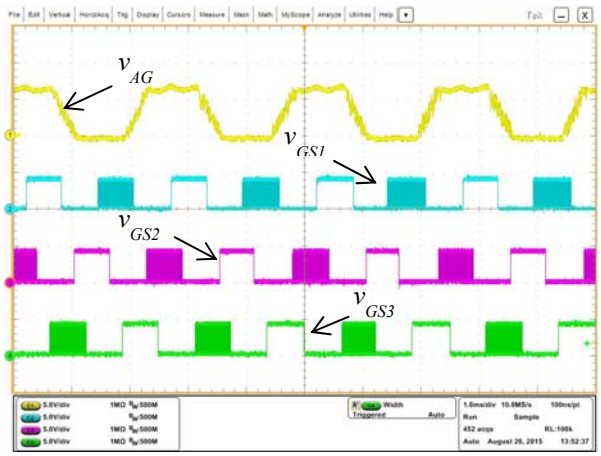

Fig. 10. From top to bottom the waveforms show the phase A input voltage referred to the ground v_{AG} waveform (5V/div) and the second, third and fourth traces show control waveforms for the inferior devices (V_{GS1}, V_{GS2}, V_{GS3}) on a three-phase boost-rectifier (5V/div and 1ms/div).

IV. IMPLEMENTATION AND EXPERIMENTAL RESULTS

Fig. 9 shows the prototype developed for the operating conditions shown in Table II. The power supply is a permanent magnet three-phase electric generator in a Y connection with a nominal peak voltage of V_{pk} =3.6 V per phase at 4500 RPM and an input frequency range between 1 Hz and 900 Hz.

Fig. 10 shows experimental control waveforms generated by the MCU according to the flow chart shown in Fig. 5 to operate the three-phase boost-rectifier in synchrony with the electric generator using the PWM HCBR modulation with the active diode scheme. For these measurements, a three-phase permanent magnet was used as the power supply.

Fig. 11 shows the voltage of phase A with respect to the ground, v_{AG}, which feeds the inverter input of the active diode on S1, the voltage of phase A with respect to the neutral (v_{AN}), the control signal from the active diode on S_1 (v_{GS1}), and the output voltage (v_0). These experimental results were obtained with a laboratory voltage supply of 3.6 V peak per phase and a

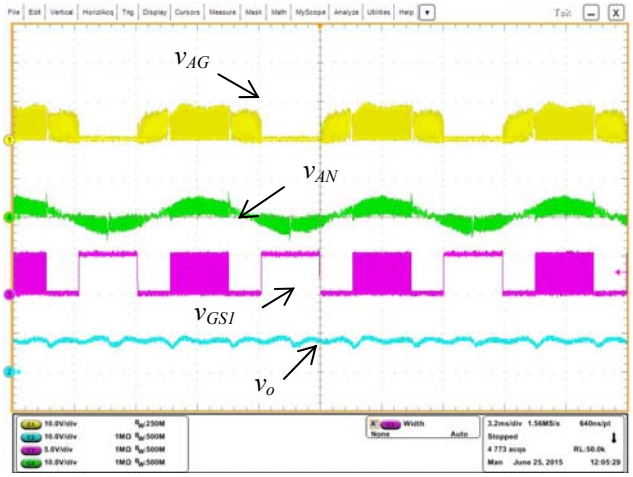

Fig. 11. From top to bottom the waveforms show the phase A input voltage referred to the ground G, v_{AG} (10 V/div), the phase A input voltage referred to the neutral, v_{AN} (10 V/div), the gate voltage on S_1, v_{GS1} (5 V/div), and the output voltage v_O (10 V/div).

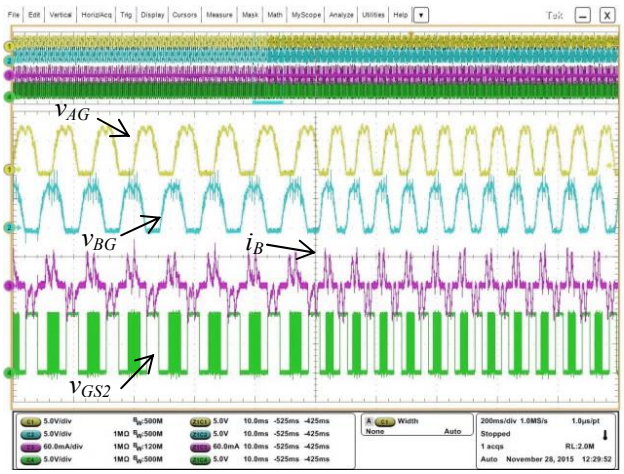

Fig. 12. The first trace shows the phase A input voltage referred to the ground, v_{AG} (5 V/div), the second trace shows the phase B input voltage referred to the ground v_{BG} (5 V/div), the third trace shows the current of phase B, i_B (60 mA/div), and the fourth trace shows the gate voltage v_{GS2} (5V/div).

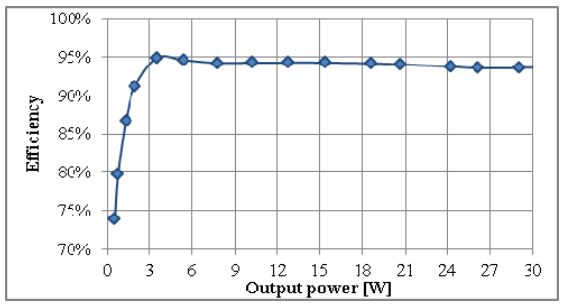

Fig. 13. Experimental efficiency for different output power conditions.

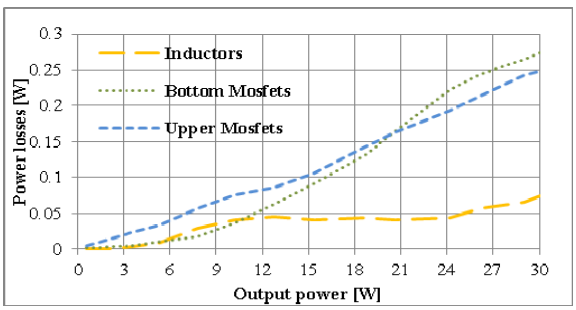

Fig. 14. Individual power losses on inductors, bottom MOSFETs (S_1, S_2, S_3) and upper MOSFETs (S_4, S_5, S_6) for different output power conditions.

TABLE V
NORMALIZED POWER LOSSES DISTRIBUTION

Component	Phase value	Total value
Upper MOSFETs (S_4, S_5, S_6)	P_{upper} = 0.72%	$P_{T(upper)}$ = 2.17%
Bottom MOSFETs (S_1, S_2, S_3)	P_{bottom} =0.84%	$P_{T(bottom)}$ = 2.51%
Input power	$P_{A,B,C}$ = 8.75 W	P_T = 26.25 W
Output power	P_0 = 24.82 W	
Efficiency	η= 94.6%	

supply frequency of 450Hz instead the three-phase permanent magnet generator. The objective was to observe the behavior of the system with a different voltage supply.

In the experimental results shown in Figs. 10 and 11 it is possible to see that the control signals v_{GS2} and v_{GS3} are always in synchrony with v_{AG} and v_{AN}. This means that there is synchrony between the three-phase boost-rectifier and the three-phase electric generator. In the other hand, v_O shows good regulation with a low frequency ripple caused by the voltage phase changes of the PWM modulation. The main advantage of making use of the active diode scheme is the control simplicity with a low computational cost when compared with typical sensorless schemes reported in the literature. Fig. 12 shows an instantaneous change of the input frequency in order to verify that the synchrony between the power converter and the permanent electric generator is kept. As can be seen, control signals keep the synchrony with the power supply.

Fig. 13 shows experimental efficiency results for different output power conditions, achieving an efficiency of up to 94.6%. In Fig. 14, the power losses for the inductors, bottom MOSFETs and upper MOSFETs are shown. As can be seen, after 20 W, the bottom MOSFETs power losses are bigger than the upper MOSFETs due to the employed PWM HCBR modulation and because the used dual channel CI (SiZ910) has different on-resistance values for the bottom and upper MOSFETs.

Table V shows the power losses distribution of the developed prototype and the efficiency obtained with the experimental results for a 24 W output power including the

power consumption of the MCU and the comparators. As Table V shows, the obtained efficiency was 94.6%. This represents an improvement when compared with the solutions reported in [3], [9]-[11]. The efficiency is kept high despite unfavorable conditions like a low voltage input (3.6 V_{pk} per phase), a high current stress on the devices and a power level greater that most of the reported energy harvesting applications.

V. CONCLUSIONS

In this paper, a sensorless self-powered scheme was proposed to synchronize the operation of a three-phase boost-rectifier with an electric generator. It has variable input frequency and voltage conditions for energy harvesting applications. The sensorless proposal is based on the active diode scheme and makes use of the gate signals from a three-phase boost-rectifier to generate a PWM HCBR modulation synchronized with the three-phase permanent magnet electric generator. The self-powered operation employs the DC output voltage from a boost-rectifier to feed the control and driver circuitry. The proposed scheme can be employed for AC generator systems like piezoelectric or MEMS with more than one phase because it extracts energy from the bigger input voltage phase no matter the waveform. Experimental results show an efficiency of up to 94.6%, which makes it a viable solution for energy harvesting applications where simplicity, low cost and high efficiency are primordial.

REFERENCES

[1] E. Lefeuvre, D. Audigier, C. Richard, and D. Guyomar, "Buck-boost converter for sensorless power optimization of piezoelectric energy harvester," *IEEE Trans. Power Electron.*, Vol. 22, No. 5, pp. 2018-2025, Sep. 2007.

[2] S. E. S., K. Chatterjee, and S. Bandyopadhyay, "One-cycle-controlled single-stage single-phase voltage-sensorless grid-connected PV system," *IEEE Trans. Ind. Electron.*, Vol. 60, No. 3, pp. 1216-1224, Mar. 2013.

[3] D. Krähenbühl, C. Zwyssig, and J. W. Kolar, "Half-controlled boost rectifier for low-power high-speed permanent-magnet generators," *IEEE Trans. Ind. Electron.*, Vol. 58, No. 11, pp. 5066-5075, 2011.

[4] D. Krähenbühl, C. Zwyssig, K. Bitterli, M. Imhof, and J. W. Kolar, "Evaluation of ultra-compact rectifiers for low power, high-speed, permanent-magnet generators," in *Annual Conference of IEEE Industrial Electronics*, 2009, No. Cm, pp. 448–455.

[5] H. J. Kim, G. B. Chung, and J. Choi, "Resonant pulse power converter with a self-switching technique," *J. Power Electron.*, Vol. 10, No. 6, pp. 784–791, 2010.

[6] G. Chung and K. D. T. Ngo, "Analysis of an AC/DC resonant pulse power converter for energy harvesting using a micro piezoelectric device," *J. Power Electron.*, Vol. 5, No. 4, pp. 247–256, 2005.

[7] S. Cheng, Y. Jin, Y. Rao, and D. P. Arnold, "An active voltage doubling ac/dc converter for low-voltage energy harvesting applications," *IEEE Trans. Power Electron.*, Vol. 26, No. 8, pp. 2258–2265, 2011.

[8] G. D. Szarka, N. McNeill, P. Proynov, and B. H. Stark, "Switched-capacitor power sensing in low-power energy harvesting systems," *Electron. Lett.*, Vol. 49, No. 2, pp. 151–152, Jan. 2013.

[9] G. D. Szarka, S. G. Burrow, and B. H. Stark, "UltraLow power, fully autonomous boost rectifier for electromagnetic energy harvesters," *IEEE Trans. Power Electron.*, Vol. 28, No. 7, pp. 3353–3362, 2013.

[10] S. S. Hashemi, M. Sawan, and Y. Savaria, "A high-efficiency low-voltage CMOS rectifier for harvesting energy in implantable devices," *IEEE Trans. Biomed. Circuits Syst.*, Vol. 6, No. 4, pp. 326–335, 2012.

[11] D. Maurath, P. F. Becker, D. Spreemann, and Y. Manoli, "Efficient energy harvesting with electromagnetic energy transducers using active low-voltage rectification and maximum power point tracking," *IEEE J. Solid-State Circuits*, Vol. 47, No. 6, pp. 1369–1380, 2012.

[12] M. Ben Said, M. W. Naouar, I. Bahri, E. Monmasson, M. Merai, M. Douma, and I. Slama-Belkhodja, "Full system on programmable chip solution for DPC control of three phase PWM boost rectifier," *IECON Proc. (Industrial Electron. Conf.*, pp. 3067–3072, 2012.

[13] H. Wu, J. Zhang, X. Qin, T. Mu, and Y. Xing, "Secondary-side-regulated soft-switching full-bridge three-port converter based on bridgeless boost rectifier and bidirectional converter for multiple energy interface," *Power Electronics, IEEE Transactions on*, Vol. 31, No. 7. pp. 4847–4860, 2016.

[14] H. Wang, Y. Tang, and A. Khaligh, "A bridgeless boost rectifier for low-voltage energy harvesting applications," *IEEE Trans. Power Electron.*, Vol. 28, No. 11, pp. 5206–5214, 2013.

[15] Y. Li, Z. Zhu, Y. Yang, and C. Zhang, "An input-powered high-efficiency interface circuit with zero standby power in energy harvesting systems," *J. Power Electron.*, Vol. 15, No. 4, pp. 1131–1138, 2015.

[16] E. Dallago, A. Danioni, M. Marchesi, V. Nucita, and G. Venchi, "A self-powered electronic interface for electromagnetic energy harvester," *IEEE Trans. Power Electron.*, Vol. 26, No. 11, pp. 3174–3182, 2011.

[17] D. Vasic, Y. Y. Chen, and F. Costa, "Design of self-powering part of SSHI interface for piezoelectric energy harvesting," *Electron. Lett.*, Vol. 49, No. 4, pp. 288–290, Feb. 2013.

[18] S. H. Song, S. Kang, K. Park, S. Shin, and H. Kim, "Applications of mems-mosfet hybrid switches to power management circuits for energy harvesting systems," *J. Power Electron.*, Vol. 12, No. 6, pp. 954–959, 2012.

[19] C. Gong, Y. Fan, Z. Wei, X. Chen, and J. Chen, "Modified one-cycle-controlled three-phase pulse-width modulation rectifiers under low-output DC voltage conditions," *IET Power Electron.*, Vol. 7, No. 3, pp. 753–763, Mar. 2014.

[20] X. Xie, C. P. Liu, F. N. K. Poon, and M. H. Pong, "The active diode - Current-driven synchronous rectifier," in *China Beijing International Power Technology Forum*, 2002.

[21] D. P. Arnold, P. Galle, F. Herrault, S. Das, J. H. Lang, and M. G. Allen, "A self-contained, flow-powered microgenerator system," *Tech. Dig. 5th Int. Workshop Micro Nanotechnology For Power Generation and Energy Conversion Apps. (PowerMEMS 2005),* 2005.

[22] M. K. Senesky and S. R. Sanders, "A millimeter-scale electric generator," *IEEE Trans. Ind. Appl.*, Vol. 44, No. 4,

pp. 1143-1149, Jul. 2008.
[23] Y. Rao and D. P. Arnold, "Input-powered energy harvesting interface circuits with zero standby power," *2011 Twenty-Sixth Annu. IEEE Appl. Power Electron. Conf. Expo.*, pp. 1992-1999, 2011.
[24] C. H. Lu, Y. J. Wang, C. K. Sung, and P. C. P. Chao, "A hula-hoop energy-harvesting system," *IEEE Trans. Magn.*, Vol. 47, No. 10, pp. 2395-2398, 2011.
[25] F. Caricchi, F. Crescimbini, O. Honorati, G. Lo Bianco, and E. Santini, "Performance of coreless-winding axial-flux permanent-magnet generator with power output at 400 Hz, 3000 r/min," *IEEE Trans. Ind. Appl.*, Vol. 34, No. 6, pp. 1263-1269, 1998.
[26] S. E. Jo, M. S. Kim, and Y. J. Kim, "Electromagnetic human vibration energy harvester comprising planar coils," *Electron. Lett.*, Vol. 48, No. 14, pp. 874-875, Jul. 2012.
[27] P. P. Proynov, G. D. Szarka, B. H. Stark, and N. McNeill, "The effect of switching frequency, duty ratio, and dead times on a synchronous boost rectifier for low power electromagnetic energy harvesters," in *2012 Twenty-Seventh Annual IEEE Applied Power Electronics Conference and Exposition (APEC)*, pp. 667-674, 2012.
[28] P. J. Grbović, P. Delarue, and P. Le Moigne, "A novel three-phase diode boost rectifier using hybrid half-DC-bus-voltage rated boost converter," *IEEE Trans. Ind. Electron.*, Vol. 58, No. 4, pp. 131-1329, 2011.

Alejandro Tapia-Hernandez was born in Mexico City, Mexico, on November 10, 1986. He received his B.S. and M.S. degrees from the National Polytechnic Institute of Mexico, Mexico City, Mexico, in 2008 and 2011, respectively; and his Ph.D. degree from the Centro Nacional de Investigación y Desarrollo Tecnológico (CENIDET), Cuernavaca, Mexico, in 2016. He is presently working as a Hardware Engineer for the R&D Instrumentation and Driver HMI in Continental Automotive, Guadalajara, Mexico, where he is working on the design of LED drivers and power supply modules for automotive clusters. His current research interests include lighting, renewable energies and power supplies for automotive applications. He has participated as reviewer for the Renewable and Sustainable Energy Reviews Journal and the European Power Electronics and Drives Journal.

Mario Ponce-Silva was born in San Luis Potosi, Mexico, on May 24, 1970. He received his B.S. degree in Electrical Engineering from the San Luis Potosi Autonomous University, San Luis Potosi, Mexico, in 1993; his M.S. and Ph.D. degrees from Centro Nacional de Investigación y Desarrollo Tecnológico (CENIDET), Cuernavaca, Mexico, in 1996 and 1999, respectively. Since March 1999, he has been working as an Associate Professor and Researcher at CENIDET. His current research interests include lighting, renewable energies, resonant converters, and power supplies for ozone generators. On these topics he has supervised 8 Ph.D., 38 M.S. and 3 B.S. degree seeking students. He is the Associate Editor of the IEEE Transactions on Power Electronics. In addition, he has participated as reviewer for the IEEE Transactions on Power Electronics, IEEE Transactions on Industrial Electronics, IEEE Transactions on Industry Applications, IEE Electronic Letters, IEE Proceedings - Science, Measurement and Technology, International Journal of Circuit Theory and Applications, International Journal of Electronics, and the Journal of Computers and Systems. He is also a Senior Member of the IEEE.

Victor Hugo Olivares-Peregrino received his B.S. degree from the Morelia Institute of Technology, Morelia, Mexico, in 1994; and his M.S. and Ph.D. degrees from Centro Nacional de Investigación y Desarrollo Tecnológico (CENIDET), Cuernavaca, Mexico, in 1996 and 2008, respectively. Since 2011, he has been a Principal in the National Center of Research and Technological Development, Cuernavaca, Mexico. His current research interests include lighting and signal processing.

Jesus Elias Valdez-Resendiz received his B.S. degree in Electronics and his M.S. degree in Electrical Engineering from Instituto Tecnologico de Ciudad Madero, Ciudad Madero, Mexico, in 2009 and 2011, respectively; and his Ph.D. degree in Electronic Engineering from the Centro Nacional de Investigacion y Desarrollo Tecnologico (CENIDET), Cuernavaca, Mexico, in 2016. He is presently a Postdoctoral Fellow at Tecnologico de Monterrey, Monterrey, Mexico. His current research interests include energy conversion systems, power converter topologies, electric and hybrid vehicles, and energy management strategies.

Leobardo Hernandez-Gonzalez received his B.S. degree in Electronics Communications Engineering and his M.S. degree in Microelectronics from the National Polytechnic Institute, Mexico City, Mexico, in 1991 and 2001, respectively; and his Ph.D. degree in Electronics Engineering in the area of Power Electronics from the National Center for Research and Technological Development (CENIDET), Cuernavaca, Mexico, in 2009. Since 1992, he has been working as a full-time Professor with Escuela Superior de Ingeniería Mecánica y Eléctrica (ESIME), National Polytechnic Institute, Mexico City, Mexico. His current research interests include the analysis and modeling of power devices, failure detection and characterization, and the design of electronic ballasts. He has participated as Reviewer for the IEEE Transaction on Power Electronics, Journal of Power Electronics (JPE), and Electric Power Components and Systems.